

H₁⁻ Production by Hydrogen Positive Ion Bombardment of a Tungsten Surface*

L. P. LEVINE† AND H. W. BERRY

Department of Physics, Syracuse University, Syracuse, New York

(Received October 2, 1959)

A study of the energy distribution of the negative ions is described. One-kilovolt ions are used. The double mass spectrograph used allows analysis of both the incoming positive- and outgoing negative-ion beams. Two peaks are studied: a low-energy peak of negative hydrogen ions created by the bombardment of a dirty surface by an assortment of positive ions, and a high-energy peak of negative hydrogen ions created only under bombardment of a surface by H₂⁺ and H₁⁺. The height of the low-energy peak is found to be proportional to the amount of hydrogen on the surface. The curve has a peak three volts wide at its half-maximum, and a tail 25 volts long on the high self-energy side. The high-energy peak ranges from zero self-energy to a value resulting from a head-on collision between a proton in the incoming ion beam and one of the atoms in the surface. This curve is flat over its whole-energy range, dropping to zero at the low self-energy end independent of incident ion energy. On a clean surface the shape of this curve is independent of target temperature.

The shape of the high-energy curve is compared with curves predicted by a random walk-collision theory and a theory based on the loss and gain, due to scattering, of particles in velocity groups. The shape of the low-energy curve is compared with curves predicted by a theory of thermal desorption of ions from a surface coupled with a mechanism for neutralization of ions as they leave the surface.

HISTORICAL ACCOUNT

Experimental Work

THE study of the negative ions formed upon positive-ion bombardment of a metal surface achieved prominence when it was seen by Massey and Smith¹ and Jen² that the cross section for formation of certain negative ions in the gas phase was far too small to account for the number of negative ions found in a gas discharge. This study was advanced by Arnot^{3,4} Sloane and Press,⁵ Sloane and Watt,⁶ and other observers.⁷⁻⁹ More recently a Russian group bombarded various metal surfaces with beams of purified positive ions, observing the formation of negative ions of various kinds, among them H₁⁻ obtained from copper, stainless steel, and aluminum.¹⁰ They noted a variation with time in the negative-ion yield after the target was flashed in vacuum. They also noted a natural width to the negative hydrogen-ion peak of the order of 10 electron volts. In their experiments, as in all previous ones, no mention was made of a peak of ions of energies greater than about 20 ev, and no mechanism for the

reflection of ions would account for the data found. The distribution of negative hydrogen ions found was more like a thermionic distribution from a source of remarkably high temperature.

Theoretical Work

The theoretical problem of the production of negative ions from incident positive ions has much in common with the associated problem of the neutralization of positive ions on a metal surface and the potential ejection of electrons. Very little work has been done on any of these problems, primarily because of the difficulty of a reasonably exact calculation. R. A. Smith,¹¹ shortly after Arnot's investigation, examined the problem from a quantum-mechanical viewpoint. While Smith was primarily interested in the Hg negative ion which Arnot thought he had found, he also performed a calculation for the formation of H⁻ from an incident H⁺ ion.

There exists a number of mechanisms by which the negative ion could be formed. Three of these, which seem to be the most important physically, are:

- (a) double resonance capture;
- (b) auger-type two-electron capture;
- (c) capture by a neutral atom.

Process a is the one which Smith examined theoretically. Figure 1(a) illustrates the process envisaged in which an ion system approaches a metal surface represented by the simple Sommerfeld model. Here ϕ is the work function, μ is the Fermi energy, V_i is the ionization energy of the ion, V_e is the ionization energy of an excited state, and W_e is the binding energy of the electron in the negative ion. The sequences of processes are shown as (1) a resonance capture of the electron into an

* Work sponsored by the Office of Naval Research.

† Now at Sperry Gyroscope Company, Great Neck, New York.

¹ H. S. W. Massey and R. A. Smith, *Proc. Roy. Soc. (London)* **A155**, 472 (1936).

² C. K. Jen, *Phys. Rev.* **43**, 540 (1933).

³ F. L. Arnot and M. A. Milligan, *Proc. Roy. Soc. (London)* **A156**, 538 (1936).

⁴ F. L. Arnot, *Proc. Roy. Soc. (London)* **A158**, 161 (1937).

⁵ R. H. Sloane and R. Press, *Proc. Roy. Soc. (London)* **A168**, 285 (1938).

⁶ R. H. Sloane and C. S. Watt, *Proc. Phys. Soc. (London)* **61**, 217 (1948).

⁷ C. H. Bachman and C. W. Carmichael, *Proc. Inst. Radio Engrs.* **26**, 529 (1938).

⁸ L. F. Broadway and H. F. Pierce, *Proc. Phys. Soc. (London)* **51**, 335 (1939).

⁹ R. H. Sloane and R. M. Hobson, *Proc. Phys. Soc. (London)* **66**, 663 (1953).

¹⁰ I. M. Mitropan and U. S. Oumenuik, *J. Exptl. Theoret. Phys. (U.S.S.R.)* **32**, 214 (1957).

¹¹ R. A. Smith, *Proc. Roy. Soc. (London)* **A168**, 19 (1938).

excited state, (2) a decay of the excited state to the ground state with this energy given to a second electron, (3) the second electron gaining sufficient energy for capture into the negative-ion bound state, and (4) the actual capture. The energy limits on the process obtained by ignoring the effect of the image force are

$$\mu + \phi > (V_i - V_e + W_e) > \phi;$$

$$\mu + \phi > V_e > \phi.$$

The effect of the image force is quite sizable, however, so that the above restrictions are at best only indicative.¹²

Smith's treatment of the process involving electron interactions that result in the formation of the negative ions requires a calculation of the transition probabilities of (1) the capture of an electron into an excited state, (2) the formation of a negative ion, and (3) the escape probability of the negative ion. The transition probabilities in each case depend on a matrix element that represents the overlap of the wave functions of the initial and final states. As such, the transition probabilities are sensitive to the choice of the form of the wave functions. In particular, where one of the states represents the electron in the metal, the result will depend markedly on the extension of the wave function for the metal electron beyond the metal surface. Of particular interest here is the calculation involving the neutralization of the negative ion as it leaves the surface. As Smith shows, this probability of escape will have a simple dependence on the velocity of the ion.

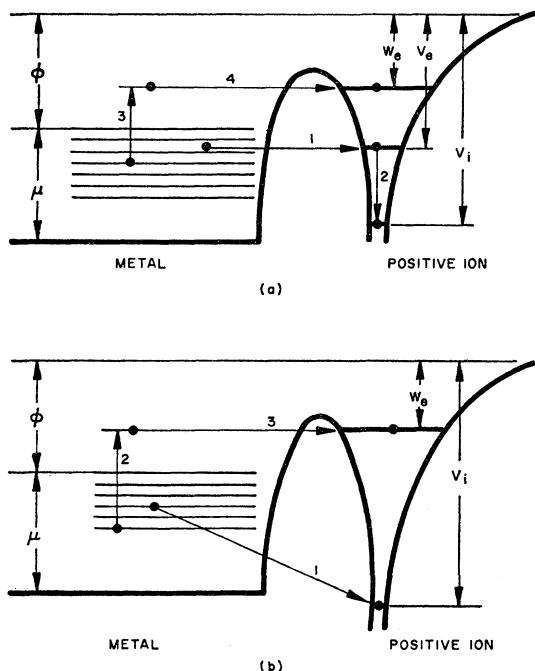


FIG. 1. Illustration of negative-ion formation processes.

¹² L. J. Varnerin, Phys. Rev. **91**, 859 (1953).

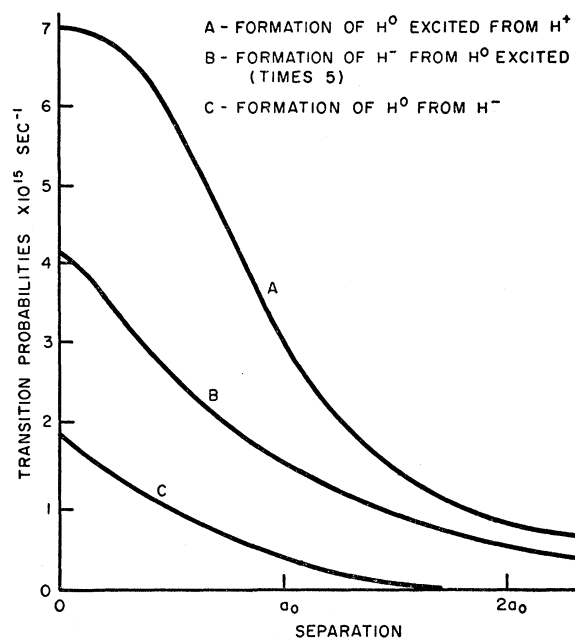


FIG. 2. Formation rates as a function of distance between the ion and metal surface.

Consequently, a measurement of the energy distribution of the "escaped" negative ions coupled with a calculated or measured initial energy distribution would yield a determination of an integrated probability. Figure 2, taken from Smith, shows this rate of neutralization as a function of the ion-metal separation as curve C. (The curves labeled A and B in this figure refer to formation rates for the excited neutral and for the negative ion, rates which are not used in our paper.)

The second mechanism listed above is shown in Fig. 1(b). Here an electron is captured directly into the ground state (1), the energy liberated is given to a second electron (2) which, if its energy is near that of the negative-ion bound state, may be captured in a resonance transition (3). The energy limitations are similar to the case above and again are subject to the sizable image-force correction.

The third process is the one of most interest here. If the negative-ion state lies below the Fermi level of the metal, a direct transition of the electron to the atom would be expected. While for hydrogen the negative-ion state has a binding energy of only 0.75 eV, it is not unlikely that the effect of the image force is to so reduce this energy of the system that the negative ion will be formed. Evidence for this will be presented in the discussion of the low-energy H⁻ ion.

THE APPARATUS

The apparatus is comprised of the following parts (see Fig. 3): a source (*S*) for the beam of ions, a lens system (*L*₁), a mass spectrograph (*M*₁) which permits the separation of the beam into one comprising ions of

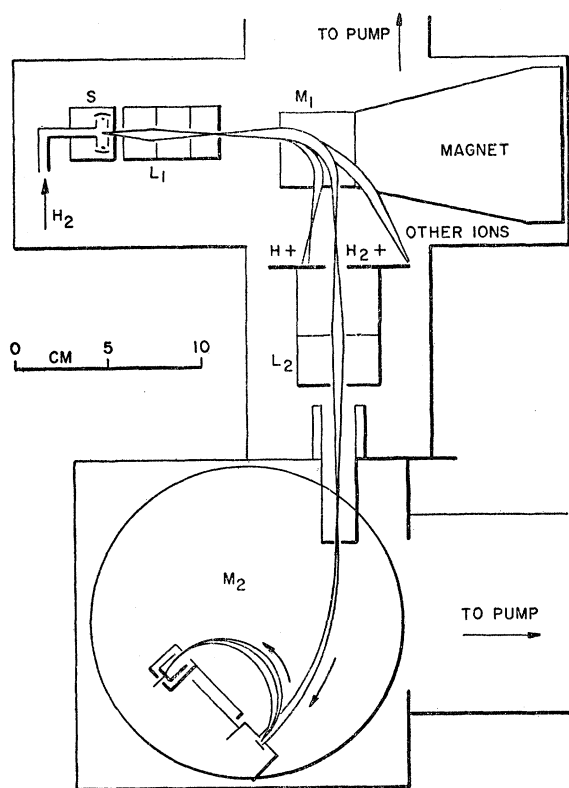


FIG. 3. Plan of experimental apparatus.

a single mass-to-charge ratio, another lens system (L_2), and finally a second mass spectrograph (M_2) with a 5-cm working radius for mass and energy analysis of the negative ions. This system, which separately analyzes the positive and negative ions, is similar to that used by Sloane and Press.

The source operates as follows.¹³ From two filaments in the source, electrons bombard the region inside a chamber with an energy of about 200 volts. A magnetic field of about 100 gauss, supplied by a small horseshoe magnet, is used to keep the electrons from being driven to the surface of the chamber too rapidly, forcing each electron to traverse the chamber several times before escaping finally to the walls. Hydrogen gas is fed into the source through a glass tube, entering the chamber from the back. The resulting ions are drawn from a hole in the front by an accelerating voltage on another electrode which is also used as a gas-retaining box. The gas used is commercial hydrogen, fed through a controlled leak into the system. It has not been considered necessary to purify the hydrogen through a palladium tube, since the resulting ions are mass-analyzed to select either protons or molecular ions, removing all other ions from the beam. The current of ions collected from this source has been as great as 100 microamperes.

The brass, electrostatic cylindrical-type lenses are

1 inch long by 1 inch in diameter. Some of the elements are split lengthwise, allowing the application of cross potentials for electrical centering. Each of our lenses is made of three such elements. In the second lens (L_2 in Fig. 3) the third element is of mild steel to afford some magnetic shielding to the positive-ion beam. In order to analyze the positive ions separately, a 90-deg mass spectrograph (M_1) with a gap width of 1 cm and pole faces 4 cm square is used.

The ion beam was observed in early measurements by means of a Willimite screen, which glowed under bombardment by ions of energies of as low as 100 volts and currents as small as 10^{-8} amp. Investigation of the beam in preliminary work showed that the energy spread of the beam was no more than 100 volts.

The electromagnet for the second mass spectrograph has a $2\frac{1}{4}$ -inch gap with 5-inch poles, and is made of mild steel. On a radius of 5 cm, there is a 5% variation of the field across the diameter of the pole. The target for the positive ions and a collector for the negative ions formed by positive-ion impact lie within the magnet gap. In front of the target is a copper accelerating electrode used to give a somewhat cylindrical form to the accelerating field. Because of the target's large, flat shape, a truly cylindrical geometry for focusing is not possible. This accelerator has been used in certain deceleration measurements discussed later. The accelerator has 0.001-inch tungsten wires strung across its face; these wires offer only a small cross section to the incoming ion beam. In front of the accelerator are the defining slits of the mass spectrograph, arranged so that they can have a maximum width of 3 mm. The target used is a tungsten ribbon $\frac{1}{8}$ inch \times 0.001 inch bent into a rectangular shape. In the system used, no portion of any insulator is visible to either the incoming positive-ion beam or to the outgoing negative-ion beam. The target can be heated by a battery-supplied heating current to a temperature of up to 2300°K, enough to drive off hydrogen gas.¹⁴ A glass-pipe, demountable vacuum system with an inside diameter of 4 inches and with O-ring grooves ground into the open ends is utilized. The use of Neoprene O-rings makes it possible to achieve pressures of the order of 10^{-6} mm of Hg. The pumps used are demountable, metal, oil diffusion pumps with a speed of the order of 200 liters per second.

In some of the later measurements with the proton beam used as the incoming ion, a source designed by Beckman was used.¹⁵ This source, much like our earlier one in that it was a crossed electron-beam source, has an extremely strong field to contain the electrons. As a result, it takes a mass spectrum of the positive ions as they leave the source. In addition, the magnetic field is shaped to allow the current density of positive ions to be increased in intensity over that which left the source. Another advantage of the Beckman source is that it allows the complicated electronics of the previously

¹³ Manfred Von Ardenne, *Physik. Z.* 43, 90 (1942).

¹⁴ J. A. Becker, *Phys. Rev.* 99, 1643 (1955).

¹⁵ L. Beckman, *Arkiv Fysik* 8, 451 (1954).

used system (source, two lenses, and one mass spectrograph) to be eliminated. H₁⁺ ions are found to leave the source we used at a positive-ion potential of 1000 v, and with a yield of protons (10⁻⁷ amp) large enough for the measurements required. No further study of this source was carried out.

THE DATA

The Low-Energy Peak

The most prominent feature of the data found is a low-energy peak of negative hydrogen ions, the peak observed by all previous experimenters in the field. During positive-ion bombardment of the target, this peak is observed if the negative-ion accelerating potential (V^-) is equal to 4.8×10^{-5} times the square of the product of the magnetic field in gauss (B) and the radius of the particle path in centimeters (R). The effective slit width in volts of this type of mass spectrograph is twice the ratio of the negative-ion accelerating potential to the particle radius times the physical slit width.

In these measurements we noted that the position of this peak never agreed exactly with our calculations. Although all the plotted curves of V^- versus B^2R^2 had a slope characteristic of the e/m of the H⁻ ion, none of these curves passed through the origin. This indicated that at the peak of the distribution, small self-energies were available, energies not supplied by accelerating potentials in the apparatus. In addition to the self-energies, there were observed varying contact potentials which made it impossible to measure the self-energy of the peak directly.

For the case of H₂⁺ ions on tungsten, a measurement was made of the yield of H₁⁻ ions in the low-energy peak as the target temperature was varied. The temperature was monitored in these runs with a thermocouple welded to the center of the target. Data were recorded as a variation of the peak height as the target was slowly heated from room temperature. A graph of these data is shown in Fig. 4. One may note two distinct features of this curve: (1) the height of the peak goes

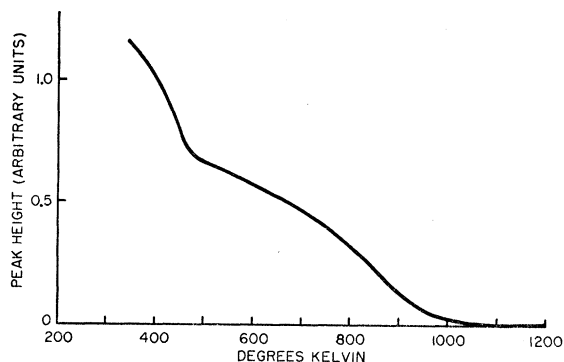


FIG. 4. Variation of the low-energy peak height as a function of the target temperature.

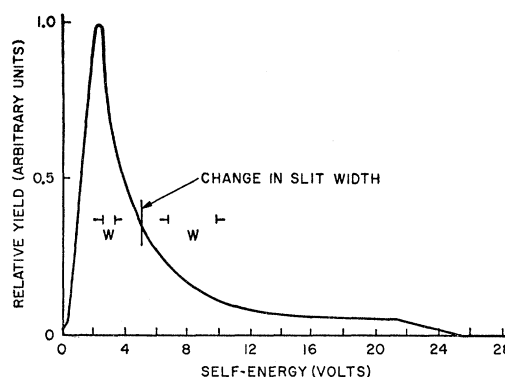


FIG. 5. Shape of the low-energy peak with the molecular hydrogen ion as the incident ion.

to zero when T is greater than 1068°K, and (2) the curve shows two inflection points, one about 480°K, and the other about 1000°K. These two points have been noted by Becker as being the temperatures at which various surface layers of hydrogen leave a clean tungsten surface.¹⁴

No information was obtained concerning the change in shape of the low-energy peak as the temperature was varied.

The low-energy peak of negative hydrogen ions was found in all cases of bombardment of a tungsten target by a positive ion. H₁⁺, H₂⁺, He⁺, and Ar⁺ were used. The relative yields were: H₁⁺, 1.4; H₂⁺, 2.0; He⁺, 4.0; Ar⁺, 10.0. The absolute yield was not measurable with our system. In all cases the low-energy peak disappeared when the target was raised in temperature to greater than approximately 1200°K. Also, in all cases, the low-energy peak returned after flashing the target.

The shape of the low-energy peak was measured with a resolving power of 0.6 ev. The curve of I^- versus self-energy is shown as Fig. 5. This curve was made by scanning across the peak, obtaining curves of increasing resolution until a value of the resolution was reached which gave no further narrowing of the peak. For H₂⁺ on tungsten, this value was reached when the slit width was 1.0 ev. As a result of the decrease in beam intensity when the resolving power was increased, the tail of the curve was not clearly measurable with a slit width of 0.6 ev. Therefore, it was taken with a slit width of 3.0 ev, and the two curves were matched at the point indicated, 2.8 volts from the peak of the curve.

The resolving power was varied by changing the potential at which H₁⁻ ions reached the collector. Since R was fixed, B was varied until a value for V^- of 15.0 volts was achieved, giving a slit width of 0.6 ev. Although the value of the negative-ion accelerating voltage was changed during a run in order to scan over a peak, the ions that reached the collector must have all had the same total energy; thus, all of the ions collected during a run must have suffered the same resolving power in spite of the change in accelerating voltage. One may note also that on the low-energy peak

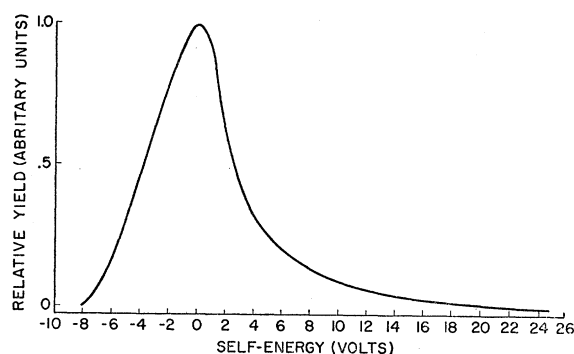


FIG. 6. Shape of the low-energy peak with the helium positive ion as the incident ion.

there exists a tail which extends to values as high as 25 volts. All of this peak, including the 25-volt tail, disappeared when the target was heated to a temperature higher than 1068°K. A measurement using He^+ ions as the bombarding ions gives a curve (Fig. 6) which, while not representing the resolving power shown in Fig. 5, does have the same general shape, the same 25-volt-long tail, and in addition, disappears at about the same value of target temperature. Because of these similarities, the two were felt to be a result of the same mechanism.

The shapes of the curves created by H_1^+ and Ar^+ bombardment were not studied, but, it was felt, would have shown nothing new.

The High-Energy Peak

The disappearance of the low-energy peak as gas was cleaned from the surface, and the production of the low-energy peak as the result of bombardment by a whole assortment of incoming ions led us to believe that the peak was the result of a sputtering process, as opposed to the rebound of individual hydrogen ions from a surface. However, during the investigation of the low-energy peak, a very long, low-intensity tail was found on the side of the peak corresponding to high self-energy. Since these measurements were made with a resolving power in the apparatus of greater than 30 volts, this is not the tail described previously. This tail extended to far higher energy and did not disappear when the target was heated. Furthermore, its energy extent was commensurate with the energy of the bombarding ion.

The shape of this high-energy peak was recorded by photographing an oscilloscope set up as an x - y recorder, using the accelerating potential on the target and the collector current as the two observables. As the target voltage was varied over the required range of several hundred volts, the incoming ion energy was of necessity also varied. As a result, a parameter Q was used,

$$Q = E_- / \frac{1}{2} E_+,$$

where E_- is the energy of the negative ion and E_+ is the energy of the positive ion, both measured simultaneously. The number one-half in this expression is used to account for the fact that the incoming particle in these experiments was a molecular ion which dissociated near the surface into two atomic particles, each with one-half the initial energy. Thus Q is the ratio of the energies of atomic particles leaving a surface to the same particles entering the surface. The value of Q measured at the high-energy end of this peak, Q_{max} , can be correlated with the rebound energy of a particle of $m=1$ atomic mass unit making a head-on collision with a stationary particle of $m=184$ amu. According to the classical laws of elastic collisions, Q_{max} is

$$Q_{\text{max}} = \frac{E_f}{E_i} = \left(\frac{m-m^*}{m+m^*} \right)^2 = 0.98.$$

For a rebound from a target of $m^*=16$ amu, this ratio is 0.78. The data found always showed a value of Q of about 1.0 on a hot tungsten surface, and around 0.8 on a gassy tungsten surface. The experimental values found were good to about 5% and always agreed with the calculated values to within one slit width. At this point we may mention another researcher, Curt Brunneé, who, upon bombarding a molybdenum surface with lithium positive ions, found a distribution of positive ions from the surface which corresponded in its highest energy to head-on collisions between lithium positive ions and molybdenum atoms with a 180-deg reversal in the paths of the lithium positive ions.¹⁶ In similar experiments with the heavier alkali metals, Brunneé found curves also terminating at the high-energy end with a value of Q_{max} computable from the expression above. Brunneé's results show that these billiard-ball collisions can explain the highest energy possible for a particle rebounding from a metallic lattice.

In order to determine if the ion peaks found were actually composed of high-energy hydrogen ions, a run was made making a simultaneous measurement of momentum and energy. The momentum was measured in the mass spectrograph and the energy of the ions was measured by placing before the target an electrode that decelerated the ions by a retarding potential U , allowing only those with an energy greater than Ue to pass through. Simultaneously, a momentum sweep was made and the resulting curve displayed on the oscilloscope. The data taken clearly showed that only the ions leaving the target with a greater self-energy than Ue were collected. In the region of momentum corresponding to lower escape energies, the yield was zero. If the high-energy peak had been composed mainly of heavy ions of low energy, as might be expected from its momentum spectrum, the deceleration would certainly have reduced the peak to zero, as it had with the low-energy peak of hydrogen ions.

¹⁶ C. Brunneé, *Z. Physik* **147**, 161 (1957).

Several runs were made over the high-energy peak at different temperatures. In most cases the high-energy peak seemed to increase in magnitude as the temperature was increased. However, this effect was not always reversible and could have been a result of the boiling off of insulating films of oil on adjacent electrodes. In all cases, however, the shape of the peak was not affected over a range of temperature from 1200°K to about 2300°K. At about 2300°K the high-energy peak of negative hydrogen ions was masked by electrons being emitted thermally from the target. No effect, other than a possible change in the magnitude of the yield, was ever observed as the temperature was varied within these limits.

Several runs were also taken over the high-energy peak for different incoming ions, namely, H₁⁺, H₂⁺, and He⁺. Most of the data taken were with H₂⁺ as the incident ion. For this ion an integrated yield of about 10⁻⁴ of the incident ion current was found. For H₁⁺, a peak was seen of about the same yield. This peak extended just twice as far as that found with H₂⁺ as the incoming particle, confirming the previous assertion that the H₂⁺ ion dissociated near the surface into two particles, each with one-half of the kinetic energy of the molecular ion. However, even with the most intense beam available for use with H₁⁺ ions, we were unable to increase the signal-to-noise ratio to the point where the shape of the H₁⁻ curve on H₁⁺ bombardment could be determined precisely. For He⁺ as the incident ion, no high-energy peak of H₁⁻ was ever seen, even with a noise level 30 times smaller than the signal height expected from the H₂⁺ measurements.

In the usual mass spectrograph data, care is taken, when quantitative results are desired, to insure that the same percentage of all ions is collected. However, in our case, as the voltage on the target relative to ground varied over the large range required to observe a peak, not only might the percentage of negative ions escaping from the target into the spectrograph vary, but also the current of positive ions to the target could vary. As a result, the data were analyzed by using only that portion of the high-energy peak which occurred when the target voltage with respect to ground was in the range of +50 to -150 volts, which was found to give the most consistent data. The curves shown in Fig. 7 were assembled in this way. They belong to five sets of positive-ion energies (E_+): (1) E_+ = 1850 to 1220 volts, (2) E_+ = 1650 to 1090 volts, (3) E_+ = 1400 to 930 volts, (4) E_+ = 1200 to 780 volts, and (5) E_+ = 1000 to 665 volts. In each case E_+ varies from the higher value at a self-energy of zero to the lower value at maximum self-energy.

In all of the curves shown H₂⁺ was the bombarding ion. In each of these curves we see that the factor Q_{\max} is: (1) 1.03, (2) 1.03, (3) 1.01, (4) 1.06, and (5) 1.01; in every case, these values are within one slit width of the appropriate value of Q_{\max} for H₂⁺ on tungsten. It is also interesting to note that the curves all drop to zero

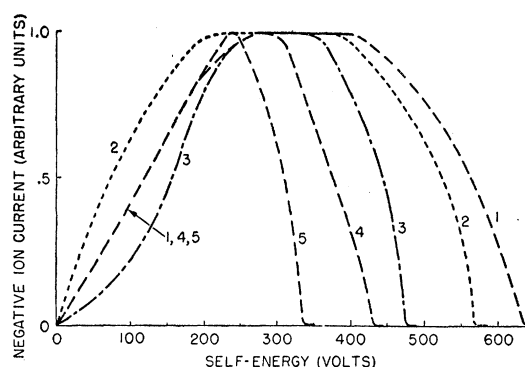


FIG. 7. Shape of the high-energy negative-ion peak.

with the same slope at a value of self-energy less than 200 volts, indicating that the shape of the curves in this region is not a function of the incident ion energy, but is instead a function of the neutralization of the negative ions as they leave the tungsten surface. This neutralization must depend only on the self-energy of the negative ions and will be discussed more fully below.

For the five curves shown, the drop-off at the high-energy end of the peaks begins at values of E_- of (1) 430 volts, (2) 400 volts, (3) 350 volts, (4) 275 volts, and (5) 225 volts. Taking the value of Q at the point where the curves just begin to drop off, we see:

$$Q_{\text{drop-off}} = \frac{E_-}{\frac{1}{2}E_+} \quad \begin{array}{l} \text{(1) 0.605} \\ \text{(2) 0.635} \\ \text{(3) 0.605} \\ \text{(4) 0.625} \\ \text{(5) 0.580} \end{array}$$

showing that the shape of the high-energy end of these curves is related to the incoming ion energy. The curves as shown in Fig. 7 have all been normalized, since from one variation of target position to another the height of the negative-ion peaks might vary by as much as a factor of five. This is caused, it is felt, by a change in the location of the positive-ion current bombardment as one changes the target position, thus affecting the yield into the spectrograph of negative ions. However, a set of four runs was taken all at one position of the target. These data may be used to give a measure of the yield at the peak of each of the high-energy curves. Relative values of the peak yield are as shown:

E_+	Yield
1000	0.57
1200	0.77
1400	0.69
1650	0.63

This shows a change in the yield per unit energy interval (dV^-) as the energy of the incoming ion is changed. Where E_+ is greater than 1200 volts, the peak height seems to go down with increasing ion energy. The value where E_+ equals 1000 volts indicates that

the peak apparently never reached its real height, but was always clipped, either by the falling off at the high-energy end or by the cutting off at the low-energy end.

It is tempting to integrate over each of the curves shown in Fig. 7 in order to get the total yield of negative ions from the surface. There is some danger in this, since in the usual experiment the integrated ion output would be made with the voltage of the incoming ions fixed. However, because of the nature of our experiment this was impossible, and the curves shown involve a simultaneous and linearly related change in the energies of the incoming and outgoing ions. In order to illustrate this we have shown a three-dimensional plot of the negative-ion yield (Fig. 8), using positive-ion energy, negative-ion self-energy, and negative-ion yield per unit negative-ion energy as the three axes. The curves shown represent the data taken. The appropriate path for a yield integration is shown by the line *A*. Such a curve could be assembled from our data if the relative heights of the respective curves were well known.

THEORETICAL ANALYSIS OF THE DATA

The low- and high-energy peaks must be treated by different mathematical techniques, and therefore will be analyzed separately.

The High-Energy Peak

Since the high-energy peak terminates at an energy that corresponds to a single collision of a proton with an atom of the target, a collision mechanism seems to be the one that would best describe it. A complete calculation of such a collision mechanism is fraught with difficulties, and an averaging system must be used if any sort of hand computation is expected. A first simplification would be to completely ignore any angular distribution. Instead, an assumption will be made that the particles rebound with an energy that is isotropic. For this case, Marshak has given an energy distribution

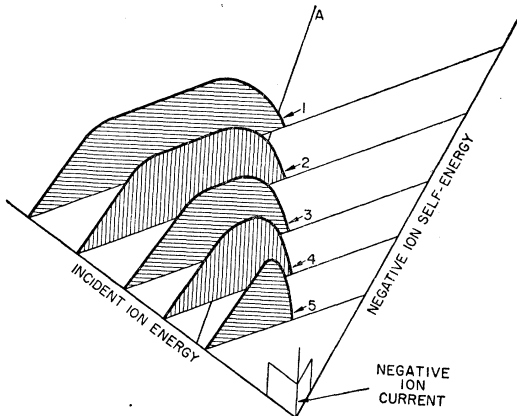


FIG. 8. Three-dimensional sketch of the negative-ion yield.

for "foreign" atoms in a lattice after n collisions.¹⁷ With this energy distribution and the probability that a particle is backscattered from the lattice after n steps, we may calculate the energy spectrum of the back-scattered particles.

The probability of backscattering is given by Chandrasekhar for the case of a one-dimensional random walk with an absorbing barrier.¹⁸ His calculation is clearly not valid for our case, since for a particle being scattered in a lattice, the probability of a forward scattering collision is just about 10 times as high as the probability of a backward scattering collision. However, the more correct problem of a random walk with a memory of the last step would be of much greater difficulty.

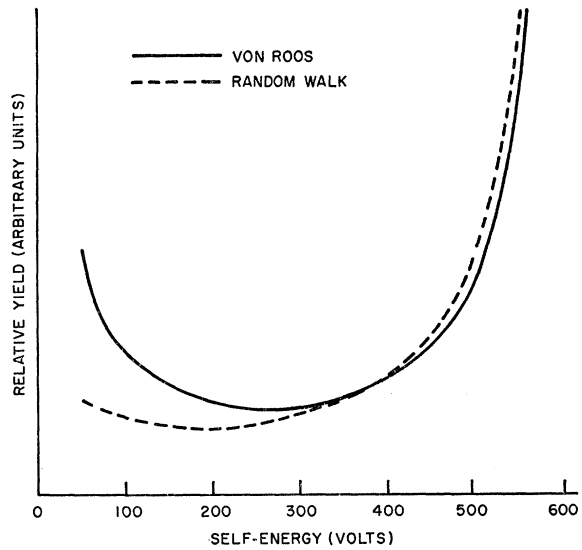


FIG. 9. Relative yield of negative ions for the von Roos and the random walk calculations.

Using the work of Marshak and Chandrasekhar, we find an energy distribution of particles scattered out of the metal after n steps for $n \gtrsim 10$. The expression may be integrated over all n , giving

$$A(u) = \frac{aq_m^{\frac{2}{3}}}{\pi^{\frac{1}{2}}} \left(\frac{(aq_m)^{2u/qm} e^{-u}}{u^{\frac{3}{2}}} \right).$$

From the definitions of terms in Marshak, we see that the energy distribution observed, $A(V)$, is just $(1/V)A(u)$; and for this experiment the flux distribution of particles from the surface has the same form as the total energy distribution,

$$\phi(V) = C \left(\frac{(aq_m)^{2u/qm}}{u^{\frac{3}{2}}} \right),$$

¹⁷ R. E. Marshak, *Revs. Modern Phys.* **19**, 199 (1947).

¹⁸ S. Chandrasekhar, *Selected Papers in Noise and Stochastic Processes*, edited by N. Wax (Dover Publications, New York, 1954), p. 9.

where C is composed of constants from the above equation. This equation is plotted in Fig. 9.

Von Roos has considered a similar problem involving the energy loss of alkali ions in a metal lattice.¹⁹ He solved the Boltzmann transport equation with approximations appropriate to a low mass ratio, and determined the distribution in velocity space within the lattice and the flux distribution of the reflected ions. If his results are applied to the case of hydrogen in tungsten, and if again the incident H₂⁺ ion energy is varied over the range of 1850 to 1220 ev to compensate for the negative-ion accelerating potential difference, then the distribution shown in Fig. 9 is obtained. It is clear from Fig. 9 that the random walk calculation and the von Roos calculation both give essentially the same curve—one that falls slightly from its value at zero reflected energy, has a flat area, and then rises sharply as Q approaches 1. This differs significantly from our data, both at the high- and low-energy ends of the curve. At the high-energy end of these curves the approximations made are poor. At the low-energy end, the data shows a gradual fall-off in yield independent of the incident ion energy. This may be correlated with the variation in the probability of escape of the negative ion (as a negative ion) as a function of the speed of the ion. (This may be compared with Brunnee's data on lithium on molybdenum where no such falling-off occurs, since essentially all lithium particles come off as positive ions.) For the case of the negative hydrogen ion we see that as protons leave a tungsten surface, they may either remain protons, be neutralized, or become negative ions. Very few remain protons; the largest number become (and remain) neutrals; and a very few become (and remain) negative ions.

Consider the process of neutralization of negative ions where $n(x)$, the neutralization rate, is a function of distance only, and N^- is the number of negative ions at a distance x . If the particles are moving at a velocity $v_x = dx/dt$, the rate of neutralization is:

$$dN^-/dx = (-N^-/v_x)n(x).$$

One may integrate over all space where negative ions may be neutralized, say from $x=b$ to $x=c$ to give

$$N^- = N_0^- \exp(-d'/v_x)$$

where

$$d' = \int_b^c n(x)dx,$$

and v_x is a constant.

For the case of formation of negative ions at the surface we must consider the rate of formation $f(x)$ per unit time also as a function of distance. Here the number formed, dN^- , depends on the number of neutral particles G :

$$dN^- = Gf(x)dt.$$

Recalling that $f(x)$ is small, we integrate from $x=a$

¹⁹ Oldwig von Roos, Z. Physik 147, 184 (1957).

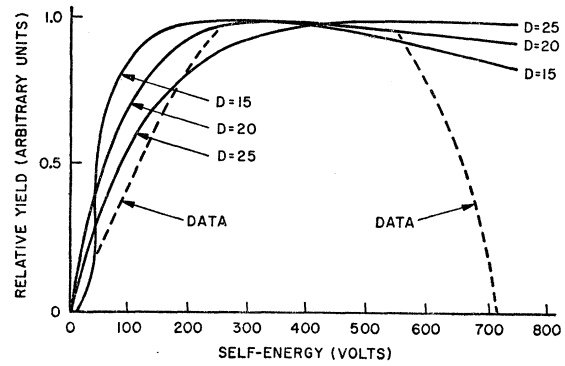


FIG. 10. Negative hydrogen ion yield for an initially flat distribution of particle velocities.

to $x=b$ giving

$$N^- = Gg'/v_x,$$

where

$$g' = \int_a^b f(x)dx.$$

If we assume that, for particles passing through the surface, negative ions are formed in the region $a < x < b$ and are neutralized in the region $b < x < \infty$, then the negative-ion yield from a surface with incident ions passing through it is:

$$\begin{aligned} N^-(v) &= Gg'(2e/m)^{1/2}(1/V^{1/2}) \exp[-(2e/m)^{1/2}(d'/V^{1/2})] \\ &= (Gg/V^{1/2}) \exp(-d/V^{1/2}), \end{aligned}$$

where

$$eV = \frac{1}{2}mv_x^2, \quad g = g'(2e/m)^{1/2}, \quad d = d'(2e/m)^{1/2}.$$

Implicit in this equation is the assumption that the formation and neutralization regions do not physically overlap. In the absence of this assumption a more complicated formula results.¹¹

If one assumes an initially flat distribution of particles through a surface, the negative-ion yield is as shown in Fig. 10 for various values of d . Note that these curves have been normalized by a variation in the value of the constant g , the integrated rate of formation. From a comparison of the data with the curves shown, it is clear that the integral, d , of the neutralization rate must have values between 15 and 30. We are able to ascribe to g a value of about 1 from the data with the value of $d=20$. This is computed from an interpolation of Brunnee's data to values suitable for hydrogen, as well as from our own data. This value of g agrees with the statement that the integrated value of the formation factor is small, since for values of V greater than 100, less than 10% of the reflected particles become ions.

The Low-Energy Peak

Formation of the low-energy peak upon bombardment by any number of different ions precludes considering it a reflection phenomenon. Furthermore, the

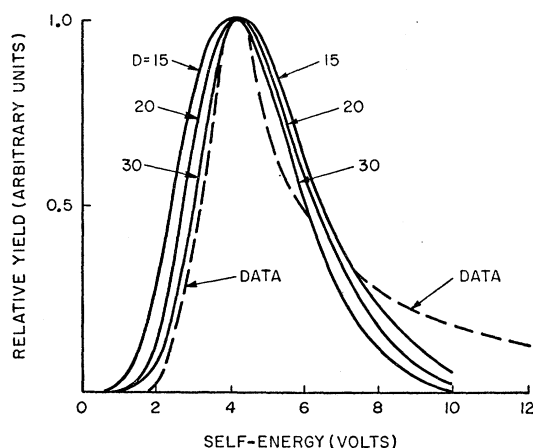


FIG. 11. Flux of ions from a heated surface compared with the low-energy peak.

rather low energies (10 eV) of these ions compared to the energies of the incoming ions makes thermal desorption of the hydrogen ions a more reasonable picture. An explanation of the phenomenon might be this: an incoming particle of any kind might transfer to the lattice a small amount of energy in each collision. This energy might be transmitted through the lattice as a wave of energy, and a negative hydrogen ion on the surface might receive it. Such an ion, vibrating at an energy corresponding to a very high temperature, stands a reasonable chance of leaving the metal surface, thereby suffering the possible loss of its extra electron according to the mechanism described in the discussion of the high-energy peak. This mechanism would not permit one to observe any yield of such negative hydrogen ions under clean surface conditions. This is in agreement with the experimentally observed fact.

In order to compute the number of ions that will escape as ions at an energy eV , consider first the equation for the flux of particles in the plane of a mass spectrometer. For a Maxwell-Boltzmann distribution from a source at a temperature T this is:

$$\phi_x = (eV/2\pi kT)^{1/2} \exp(-eV/kT).$$

Multiplying this equation by the neutralization factor described in the previous section, one finds the ion-flux curves which have been plotted as Fig. 11. The curves plotted are for values of d of 15, 20, and 30 and for values of T of 11 500°K, 9000°K, and 6800°K, respectively. Superimposed on them is the curve representing the actual data. We note the following: the curves plotted all have a half-width of 3 eV. The curves all peak at 4 volts of self-energy. The data curve peaks at a value of 2 volts from its onset point, although its self-energy in absolute units could not be determined because of contact potential difficulties. In general in the region around the peak of the distribution, the curves plotted agree rather nicely with the data. However, the data curve has a tail of high-energy particles extending to about 25 volts of self-energy, unlike any of the curves that could have been plotted according to this model of high-temperature negative-ion evaporation. The long, rather flat tail is due to some undetermined mechanism.

The area under curve C of Fig. 2 is the integrated probability of neutralization of the hydrogen negative ion leaving the metal surface. This, expressed in volts to the one-half power corresponding to the d in Fig. 10 and 11, is about 5.0. It would thus appear that the calculation yields a value for this interaction which is low by a factor of three or four, if the simple analysis of the experimental results presented here is accepted.

Thus it seems from the above analysis that the data can be explained in terms of a collision process for the high-energy peak of negative ions, and a process of thermal desorption for the low-energy peak of negative ions, coupled with a rather simple mechanism for the formation and neutralization of negative ions at a metal surface. These calculations give values for the formation integral and neutralization integral which are consistent and reasonable in size. The calculations which have been performed are admittedly crude and do not fit the data in all details, but do offer some clue to the mechanism of an ion-lattice interaction as well as surface sputtering effects.